

Lattice Free Stochastic Dynamics

Alexandros Sopasakis*

Center for Mathematical Sciences, Lund University, Box 118, 22100 Lund, Sweden.

Received 11 February 2011; Accepted (in revised version) 20 June 2011

Communicated by Wei Cai

Available online 1 March 2012

Abstract. We introduce a lattice-free hard sphere exclusion stochastic process. The resulting stochastic rates are distance based instead of cell based. The corresponding Markov chain build for this many particle system is updated using an adaptation of the kinetic Monte Carlo method. It becomes quickly apparent that due to the lattice-free environment, and because of that alone, the dynamics behave differently than those in the lattice-based environment. This difference becomes increasingly larger with respect to particle densities/temperatures. The well-known packing problem and its solution (Palasti conjecture) seem to validate the resulting lattice-free dynamics.

AMS subject classifications: 82C20, 82C22, 82C80, 82B20, 82D99, 90B20

Key words: Lattice-free, microscopic stochastic dynamics, kinetic Monte Carlo.

1 Introduction

Stimulated by the exponential growth in CPU power computationally intensive models and applications have thrived in recent decades. Among them lattice models through Cellular Automaton (CA) and/or Monte Carlo methods have proliferated significantly and are increasingly used to describe and understand a wide variety of complex physical and biological systems [25]. CA for instance have been used in modeling gas phenomena, urban development, immunological processes, and crystallization. The best known application for CA is modeling living systems [26].

Lattice models in conjunction with Monte Carlo methods are often [15] used as a way of modeling systems involving many interacting particles under the influence of noise. Such approaches have been followed in many fields although they are particularly responsible for significant innovation in space and oil exploration [6]. Similarly, molecular dynamics modeling through lattice gas CA or lattice Boltzmann methods are responsible

*Corresponding author. *Email address:* sopasak@maths.lth.se (A. Sopasakis)

for producing a better understanding for a number of fundamental scientific problems in the physics of fluids.

A lattice based model describes a particle system by introducing a spatial discrete lattice consisting of predetermined number of cells within which the particle interactions and dynamics will evolve. One common approach is to build a Markov Chain which evolves the dynamics responsible for constructing the solution of the system. The stochastic dynamics applied depend on the physical properties describing the microscopic interactions for the system. As a result, Metropolis, Arrhenius, Glauber, Kawasaki and other rates are carefully considered depending on the knowledge of the microscopic behavior of the system. The applications of such methodologies range from granular material [14, 19], traffic flow [22], ecology [5, 7], lattice Boltzmann and lattice gas [23, 27], surface growth [13] just to name a few.

In this work we construct a lattice-free (LF) stochastic process. The underlying stochastic dynamics are stripped of their dependence on the usual lattice-based (LB) environment. Interacting particles therefore will be free to land and interact at locations prescribed by the dynamics from stochastic rates which are distance based instead of cell based. For this exposition we equip our stochastic process with an Arrhenius spin-flip (non-conservative), hard sphere, exclusion potential and examine/compare the particle behavior at equilibrium as well as on the transition path to equilibrium. Other potentials can also be considered as well since the findings of this work are not tied to the particular form of the interaction potential used. We furthermore propose a corresponding version of the well-known kinetic Monte Carlo (KMC) algorithm in order to practically implement this LF stochastic process. Although we restrict our exposition in this article to updates performed by the KMC algorithm other updating mechanisms can also be considered and applied in a similar fashion.

We motivate the application of LF dynamics by exposing obvious shortcomings in solutions produced by LB dynamics under certain regimes where particle sizes can influence or interfere with their interactions. Under such regimes LB dynamics and corresponding LB models can produce erroneous results with non-physical solutions. This phenomenon occurs for all interaction potentials. The differences in solutions however are most pronounced for model parameters promoting high particle densities. Furthermore, we show that convergence will not fix this discrepancy. In other words, as the lattice size increases the solutions from LB dynamics will not converge to that of the LF dynamics. Clearly the reason for the difference in solutions between LB and LF dynamics simply results from the fact that a lattice, with predefined cells for particles to land in, offers a more efficient use of space. As a result the corresponding density of those particles can be much higher in the case of LB models. Many natural processes involve interactants which move in continuum space and not in preset distances/cells as is the case for LB environments. Thus in several modeling situations such a LB methodology, although easier to implement, will produce wrong solutions.

2 Lattice free stochastic process

We now provide all the details towards the construction of the LF microscopic stochastic process. We let $\Lambda = \mathbb{T}^d$ where $\mathbb{T}^d = [0,1)^d$ is a d -dimensional torus and d denotes the spatial dimension. For contrast we note that for a typical two-dimensional LB stochastic process the corresponding lattice Λ consists of a predetermined number of microscopic cells all of which have the exact same dimensions and each of which could accommodate a single particle.

For now we assume that all particles occupy the same volume $B_i = B_r(\vec{x}_i)$ with radius r around their centers $\vec{x}_i \in \Lambda$ and that physically it will not be possible for two particles to occupy the same space. This will be implemented below using an exclusion principle.

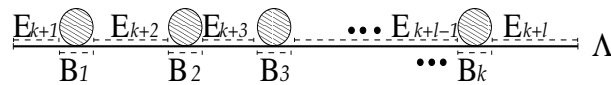


Figure 1: Schematic of disjoint sets comprising Λ for one-dimensional example. E_i 's denote unoccupied space and vary in size. B_i 's denote occupied space by a single particle and their size is the same as that of the particle.

We let the domain be comprised of a number of disjoint sets $\Lambda = P \cup P^C$. Here $P = \cup B(\vec{x}_i)$ for $i = 1, \dots, k$ and $P^C = \cup E_i$ for $k+1 \leq i \leq k+l$ where E_i denotes all the disjoint unoccupied sets in Λ . Note that the size of the E_i 's can differ since each E_i denotes the empty space between particles with centers at x_i and x_{i+1} , i.e. $|E_i| = |x_{i+1} - x_i| - 2r$. In contrast the size of the B_i 's is the same. In one-dimension for instance each $B_i = B_r(\vec{x}_i)$ corresponds to a line segment occupied by a particle (see Fig. 1). In two-dimensions of course all such sets B_i 's, E_i 's represent areas. Note therefore that the lattice Λ can always be represented as a set of a finite number of such empty and filled sets,

$$\Lambda = P \cup P^C = B_1 \cup B_2 \cup \dots \cup B_k \cup E_{k+1} \cup \dots \cup E_{k+l}$$

even as those sets will be changing while the particles move and occupy different locations over time.

The degrees of freedom (the microscopic order parameter) is given by a spin-like variable $\sigma(i)$ for $1 \leq i \leq k+l$ for each set B_i or $E_i \in \Lambda$. In this work we present only the case of discrete spin variables although generalizations to the continuous case (Heisenberg model) can be carried through without major changes. We start by defining a microscopic stochastic process $\{\sigma\}_i$ and define each $\sigma(i)$ to occupy a volume equivalent to the particle volume it is supposed to represent. Specifically

$$\sigma(i) = \begin{cases} 1, & \text{if there exist a particle at } i, \\ 0, & \text{if there is no particle at } i, \end{cases}$$

where $1 \leq i \leq k+l$.

We denote the configuration of spins on the lattice by $\sigma = \{\sigma(i) | 1 \leq i \leq k+l\}$. A spin configuration σ is an element of the configuration space $\Sigma = \{0,1\}^N$ where $N = |\Lambda| = k+l$.

The interactions between spins are defined by the microscopic Hamiltonian,

$$H(\sigma) = -\frac{1}{2} \sum_{i=1}^{k+l} \sum_{j=1}^{k+l} J(i-j) \sigma(i) \sigma(j) + \sum_{i=1}^{k+l} h_i \sigma(i), \quad (2.1)$$

where $h_i = h(\vec{x}_i)$ denotes the external field at \vec{x}_i . We note that this Hamiltonian is not used directly towards the construction of the Markov chain however. Instead, for that purpose, we make use of the local, hard sphere type, interaction potential J

$$J(i-j) = \frac{1}{(2L+1)^d} V\left(\frac{1}{2L+1} |\vec{x}_i - \vec{x}_j|\right), \quad 1 \leq i \leq k+l, \quad (2.2)$$

where we let $V: \mathbb{R} \rightarrow \mathbb{R}$ with $V(s) = V(-s)$ and $V(s) = 0$ if $|s| \geq 1$. In fact for simplicity we take $V(s) = J_0$ for $|s| \leq 1$. For now we assume uniform potentials and let J_0 to be a constant. The interaction radius for these dynamics is denoted by L in (2.2). Note that due to the construction of V the potential in (2.2) and corresponding Hamiltonian (2.1) will be well defined and summable even in the case of $N, L \rightarrow \infty$. The canonical equilibrium state for the stochastic process $\{\sigma_t\}_{t \geq 0}$ is given by the Gibbs measure [15]

$$\mu_\beta(\sigma) = \frac{1}{Z_\beta} e^{-\beta H(\sigma)} P(d\sigma), \quad (2.3)$$

where $\beta = 1/kT$ is the inverse temperature and k is the Boltzmann constant. Here Z_β is the normalizing partition function and $P(d\sigma) = \prod_{\vec{x} \in \Lambda} \rho(d\sigma(\vec{x}))$ the a priori Bernoulli product measure. Typical choice for ρ in Ising systems would be $\rho(0) = \rho(1) = 1/2$.

3 Arrhenius spin-flip dynamics

Depending on how particles interact we can equip the stochastic process σ with a number of different dynamics. In Ising systems for instance Metropolis dynamics are applied with rate

$$c(i, \sigma) = \Psi(-\beta \Delta_{\vec{x}_i} H(\sigma)),$$

where

$$\Delta_{\vec{x}_i} H(\sigma) = H(\sigma^{\vec{x}_i}) - H(\sigma)$$

with Ψ a continuous function satisfying $\Psi(r) = \Psi(-r)e^{-r}$, $r \in \mathbb{R}$ [3, 15]. Other common choices for Ψ can be Glauber $\Psi(r) = (1 + e^r)^{-1}$, Kawasaki, Barker, etc [15]. The type of dynamics chosen is of great importance for the proper description of the underlying physical process. In Metropolis dynamics for instance the choice to perform a spin-flip [15] depends on the *energy difference* between the initial and final states of the process. On the other hand in Arrhenius dynamics the activation energy of spin-flip is defined as the *energy barrier* a species has to overcome in jumping from one phase to another. These rates are derived from transition state theory or molecular dynamics calculations.

For this work we implement Arrhenius spin-flip dynamics although we will consider other rates [8, 12] in the future. Such dynamics are usually associated with desorption or adsorption of particles from and to a surface [11, 13]. For traffic flow [22], for instance, such non-Hamiltonian dynamics are responsible for adding or removing vehicles from the highway at select locations while in micromagnetics they are responsible for changing the overall magnetization of the surface according to a prescribed temperature [10].

The rate by which spin-flip dynamics evolve particles in a LF domain is given by

$$c(i, \sigma) = \begin{cases} c_d \exp(-\beta U(i, \sigma)), & \text{if } \sigma(i) = 1, \\ c_a w(i), & \text{if } \sigma(i) = 0, \end{cases} \quad (3.1)$$

for $1 \leq i \leq k+l$. Here $w(i)$ is a weight function related to the empty space still available for particle adsorption at location i in the domain. The exact details for $w(i)$ will be provided below in (4.1). Here c_a and c_d denote adsorption and desorption constants respectively and involve the inverse of the characteristic time of the stochastic process. Usually c_a and c_d are calibrated from experimental parameters such as particle velocities or reaction times. The potential function in (3.1) is given by [9, 15] $U(i, \sigma) = \sum_{j=1}^{k+l} J(i-j)\sigma(j) - h_i$ with J from (2.2). We point out that based on definition (3.1) if there is already a particle located at i then we have $\sigma(i) = 1$ and therefore we can not adsorb at that location since the rate $c(i, \sigma)$ in (3.1) only allows desorption from such a location. Thus exclusion principle is enforced.

The stochastic process $\{\sigma_t\}_{t \geq 0}$ is a continuous time jump Markov process on $L^\infty(\Lambda; \mathbb{R})$ which evolves with the rule [15], $\frac{d}{dt} \mathbb{E}f(\sigma) = \mathbb{E}\mathcal{L}f(\sigma)$. Here \mathbb{E} denotes the expected value with respect to the equilibrium measure μ_β from (2.3), $f \in L^\infty(\Lambda; \mathbb{R})$ is a test function and \mathcal{L} denotes the generator for this stochastic process [15]

$$\mathcal{L}f(\sigma) = \sum_{i=1}^{k+l} c(i, \sigma) [f(\sigma^{\bar{x}_i^*}) - f(\sigma)],$$

where \bar{x}_i^* denotes the configuration after the spin has changed (flipped) at \bar{x}_i . Detailed balance $c(i, \sigma) \exp(-H(\sigma)) = c(i, \sigma^{\bar{x}_i^*}) \exp(-H(\sigma^{\bar{x}_i^*}))$ ensures that the invariant measure for this process is the Gibbs measure prescribed by (2.3).

4 Lattice-free kinetic Monte Carlo

Monte Carlo methods are used for a variety of scientific applications. Systems can be simulated for up to 10^{10} mesh points for some specialized computer architectures. In many cases however critical slowing down occurs when the dynamics reach equilibration thus even Monte Carlo approaches become computationally expensive.

Among the many choices for numerically updating stochastic dynamics the KMC algorithm [2, 4] or n -fold way is prominent since there is no slowing-down effect at the process nears equilibration. In that respect every move performed by the KMC algorithm results in a success. Under the KMC update particles perform moves at every time

iteration regardless of whether the system is near equilibration or not. As a result KMC is a favorite in the literature since it avoids excessive computational overhead due to this critical slowing down phenomenon which can be detrimental for typical Monte Carlo methods.

We now present a generalization of the original KMC algorithm [2] adapted to accommodate this new LF stochastic process. The driving force behind the updating of the stochastic dynamics is in the calculation of the rates for adsorption to, or desorption from, the domain. The rates for desorption for each particle on the domain can be calculated directly from (3.1). The rates for adsorption however depend on the amount of unoccupied space on that domain. In classic LB KMC algorithms the adsorption rates are calculated for each unoccupied lattice cell with weight $w(i) = 1$. In our case we obtain the adsorption rates by first identifying all the available unoccupied space, E_i 's, within the domain. We then calculate the adsorption rate with a weight corresponding to the amount of empty space found. In the one-dimensional case for instance

$$w(i) = \begin{cases} |E_i| - 2r, & \text{if } |E_i| > 2r, \\ 0, & \text{otherwise.} \end{cases} \quad (4.1)$$

This implies that if the size of the empty space between two adjacent particle locations is not large enough then the corresponding adsorption rate is 0 and no particle has a chance of landing there (exclusion principle). This is enforced through the stochastic rate $c(i, \sigma)$ in (3.1).

Note that although the domain is continuous (not a lattice) the rates (3.1) will always be countable. The stochastic process developed above therefore is not just an abstract mathematical object but can also be constructed as shown in the pseudo-code provided in the Appendix. This pseudo-code gives only a rough outline of the main algorithm. There are several techniques, not listed here, which allow for significant speed-up for each of the main steps presented in the Appendix. We also note that there are a number of recent improvements [20, 21] for the original KMC algorithm which can also be implemented in this LF KMC. These techniques would allow for significant speed-up and further computational efficiency.

4.1 Adsorption location

The only remaining question therefore is how the dynamics pinpoint the exact location on the domain at which such a particle will adsorb to. That location is calculated through the invariant measure μ_β from (2.3) as shown below.

We note that for Arrhenius dynamics a spin is flipped as long as the rate (energy barrier) has been overcome. Sampling for instance from μ_β under the detailed balance condition we choose a random rate c^* as follows $0 \leq c^* \leq \sum_{i=1}^{k+1} c(i, \sigma)$. Assume for instance

$$\sum_{i=1}^{m+1} c(i, \sigma) > c^* \geq \sum_{i=1}^m c(i, \sigma),$$

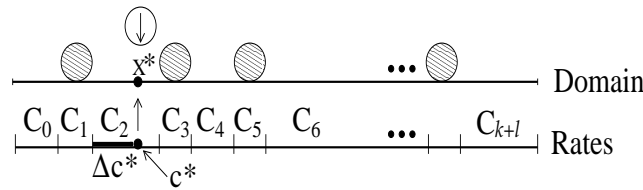


Figure 2: Adsorption at x^* for one-dimensional example. The rates c_i for each location in this LF domain are calculated from (3.1) depending on whether the domain is occupied by a particle or not. The adsorption location x^* is then obtained from (4.2).

for some $0 \leq m < k+l$. Then in classic LB methods a particle would adsorb at lattice cell m . LF dynamics do not involve such boundaries however. LF dynamics will instead adsorb at location \bar{x}^* corresponding to the exact rate c^* (see Fig. 2). In the one-dimensional case for instance

$$x^* = \Delta c^* / c_a + 2r, \tag{4.2}$$

where $\Delta c^* = c^* - \sum_{i=1}^m c(i, \sigma)$. Similar calculations can be performed in higher dimensions as well. Stochastic dynamics are therefore updated with a KMC pseudo-code for LF domains whose details are provided in the Appendix.

To further facilitate the mathematical analysis of our stochastic dynamics we consider an analogue of the Curie-Weiss model where we allow long-range uniform, weak interactions. The Curie-Weiss spin model is a classic simple example in statistical mechanics that exhibits phase transitions even in one-dimension and further allows for detailed calculations such as mean field and thermodynamical limit at all temperatures. As the domain size approaches infinity and particle radius $r \rightarrow 0$, under appropriate scaling and limit arguments [9,24], the coverage c can be shown to solve the following equation

$$c_t - \nabla \cdot F = 0 \tag{4.3}$$

with flux function $F = c_0 [\nabla c - \beta c(1-c) \nabla J * c]$ where $J * c$ denotes a convolution. A similar such derivation can be obtained for Metropolis type dynamics [24].

5 Monte Carlo simulations

In the simulations which follow we present results of LB and LF stochastic processes under the influence of spin-flip dynamics using Monte Carlo simulations in one-dimension. We apply circular boundary conditions: as the lattice ends on one side it is continuous on the other side. Other types of boundary conditions can easily be implemented as well without difficulty. Simulations for higher dimensions will be carried out in the future.

We provide comparisons for LB versus LF dynamics in Fig. 3. Three examples are presented in that figure based on different choices of the temperature parameter $\beta J_0 = -2, .01, 3$ for repulsive, (almost) neutral and attractive dynamics respectively. We know [9, 10] that for $\beta J_0 = -2, .01, 3$ the average density for LB dynamics should be approximately .34, 0, .94 respectively.

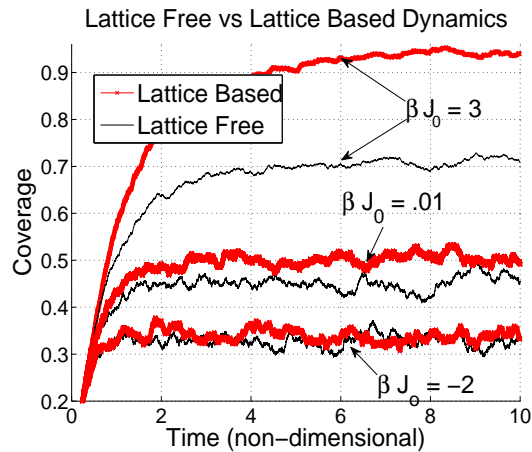


Figure 3: Three examples for $\beta J_0 = 3, .01, -2$. Dynamics compared pathwise and at equilibration. The case of $\beta J_0 = -2$ does not show any obvious discrepancy. Any positive temperature however $\beta J_0 > 0$ will involve significant errors if LB dynamics are used. The case $\beta J_0 = 3$, for instance, promoting high particle densities, produces significantly different dynamics. Compare with simulations in Fig. 4 and extended results in Table 1.

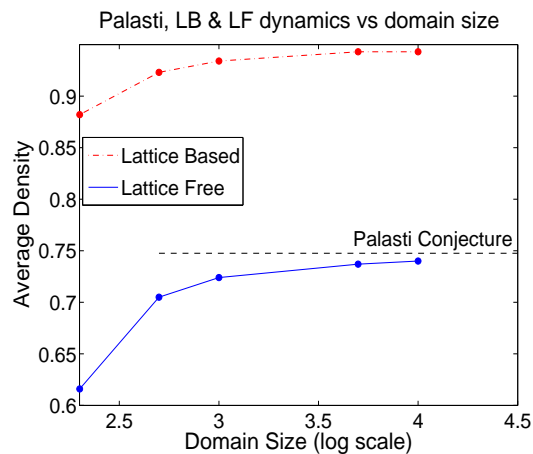


Figure 4: Comparison of ensemble average coverage for $\beta J_0 = 3$ versus domain size for the classic LB dynamics versus the new LF dynamics. Each point corresponds to ensemble, uncorrelated, density averages \bar{c} after equilibration. The LF dynamics seem to respect the Palasti conjecture.

However the results in Fig. 4 and especially in Table 1 show disagreement between LB and LF dynamics for all values of βJ_0 . The difference in solutions is quite significant for the case of $\beta J_0 = 3$. The case of $\beta J_0 = 3$ corresponds to high particle densities. In fact, as presented in the more detailed study in Table 1, all temperatures $\beta J_0 > 0$ would fall into that category with increasing discrepancies for higher particle densities and corresponding increasingly higher differences in the dynamics. In Table 2 further long-time ensemble averages are calculated for the case $\beta J_0 = 3$ in order to better understand this discrepancy between LB and LF dynamics as domain size increases.

Table 1: The average density $c = \frac{1}{k+1} \sum \sigma(x)$ in one-dimension for a range of βJ_0 values. Averages are provided over several uncorrelated ensembles. Note that the LB density is clearly different than the LF dynamics. The errors increase as temperature βJ_0 (and particle density) increases.

βJ_0	-10	-3	-2	-1	0	1	2	3	10
Density(LB)	.189	.295	.336	.486	.504	.663	.835	.945	.997
Density(LF)	.174	.287	.325	.439	.449	.549	.649	.743	.744
Rel. Errors (%)	3	3	3	9	11	17	22	22	>22

Table 2: The average density $c = \frac{1}{k+1} \sum \sigma(x)$ in one-dimension for $\beta J_0 = 3$ as domain size increases. Averages over several ensembles. Results shown in Fig. 4. The LB density is clearly different than the LF dynamics regardless of domain size. Convergence will not fix that difference. The theoretical estimate (6.1) for domain size $N \rightarrow \infty$ is $c = .74759$ which supports the LF solution.

Domain Size	200	500	1000	5000	10000	20000
Density(LB)	.882	.923	.934	.941	.942	.945
Density(LF)	.616	.705	.724	.736	.740	.743

6 Discussion

A theoretical result from Renyi [18] as well as the well-known conjecture due to Palasti [17] further validate our findings since it is shown [18] that as the line becomes infinite in length the packing density c_* of randomly placed unit intervals is

$$c_* = \int_0^\infty \exp \left\{ -2 \int_0^t \frac{1 - e^{-u}}{u} du \right\} dt = .74759. \tag{6.1}$$

This theoretical value is in agreement with the numerical solutions obtained in Fig. 4 for $\beta J_0 = 3$ as well as the extended results shown in Table 2. It is clear from Table 2 that for the full range of temperatures $-10 \leq \beta J_0 \leq 10$ we have obtained a similar upper bound which agrees with this conjecture. The Palasti conjecture further states that in n-dimensions the random packing density of unit squares would be c_*^n [17].

We have shown that the dynamics are clearly different between LB and LF processes (see Fig. 4). We found that if traditional, LB dynamics, are used to model physical processes which evolve continuously in space then erroneous solutions can result for all values of βJ_0 . These errors become larger with increasing βJ_0 as shown by the relative errors in Table 1. In this case statistical estimates of densities from LB dynamics are always greater (and wrong) than those of LF dynamics. The relative errors presented in Table 1 become significant as soon as $\beta J_0 > 0$. Furthermore, as has been shown in Fig. 4, increasing the lattice size and/or number of interacting particles will not diminish these errors.

This work therefore points out some of the issues resulting due to the fact that for a number of models particle size is actually important towards understanding system behavior. So the main point which we advocate here is that in many physical applications

significant errors can occur if we disregard the effects due to particle size. The problem arises because in many instances particles modelled with such lattice dynamics actually have significant (non-negligible) size in relation to their domain and therefore it is not physically meaningful to take the limit as the lattice cell gets smaller and smaller. If however particle size is not significant in the corresponding physical system we model then both LF and LB dynamics will produce the same continuum PDE in the limit of particle size or corresponding cell size reaching 0 as shown in (4.3).

Our findings have direct consequences in the modeling of a number of physical applications for which LB models have been used inappropriately (i.e for modeling particles of non-negligible size). A large amount of work in CA simulations for instance comes into question due to the fact that LB dynamics seem to produce wrong solutions at high concentrations. CA simulations of traffic flow for instance is the predominant [1, 16] methodology of solutions especially during high vehicle concentrations. According to our findings such simulations should not be trusted for the simple reason that actual vehicles do not move in lattice cells (even if safe distances are included). Similar such examples exist in many other fields where LB dynamics have been applied to model continuous spatial interactions at high densities. In such cases therefore LB dynamics should not be applied. In particular the size of the lattice can not and should not be considered as cell size goes to 0 if particle sizes are important towards understanding the behavior of the actual physical system we try to model. The LF process proposed here could potentially be used instead to eliminate such discrepancies.

Appendix: Pseudo-code for lattice-free Monte Carlo dynamics

The LF KMC algorithm for Arrhenius spin-flip dynamics is provided below.

1. Calculate all transition rates for adsorption $c^a(l)$ and desorption $c^d(l)$ from (3.1) for the domain Λ .
2. Calculate the total rates to adsorb $R_a = \sum_l c^a(l)$ or desorb $R_d = \sum_l c^d(l)$. Obtain the total rate $R = R_a + R_d$.
3. Obtain a random number ρ . Index rates in an array c .
4. Find j and x^* for which $\sum_{j=0}^m c(j) \geq \rho R > \sum_{j=0}^{m-1} c(j)$.
5. Update the time, $t = t + \Delta t$ where $\Delta t = 1/R$.
6. Repeat until dynamics of interest have been captured.

Acknowledgments

The author acknowledges the support of Prof. Stig Larsson at the Mathematics Department and SAFER at Chalmers Institute of Technology where part of this work was completed. The computations were performed on C3SE computing resources at Chalmers.

References

- [1] O. Biham, A. A. Middleton, and D. Levine. Self-organization and a dynamical transition in traffic-flow models. *Phys. Rev. A*, 10:6124, 1992.
- [2] A. B. Bortz, M. H. Kalos, and J. L. Lebowitz. A new algorithm for Monte Carlo simulations of Ising spin systems. *J. Comput. Phys.*, 17:10, 1975.
- [3] B. Gidas. Metropolis-type Monte Carlo simulation algorithms and simulated annealing. In J. Laurie Snell, editor, *Topics in Contemporary Probability and its Applications*. CRC Press, 1995.
- [4] D. T. Gillespie. A General Method for Numerically Simulating the Stochastic Time Evolution of Coupled Chemical Reactions. *J. Comput. Phys.*, 22:403, 1976.
- [5] S. M. Henson, R. F. Costantino, J. M. Cushing, R. A. Desharnais, B. Dennis, and A. A. King. Lattice effects observed in chaotic dynamics of experimental populations. *Science*, 294:602–605, 2001.
- [6] D. Hubbard, *The Failure of Risk Management: Why It's Broken and How to Fix It*, John Wiley & Sons, 2009.
- [7] E. A. Jackson. *Perspectives of nonlinear dynamics*. Cambridge Univ. Press, 1:216–219, 1989.
- [8] M. A. Katsoulakis, A. J. Majda, and A. Sopasakis. Multiscale couplings in prototype hybrid deterministic/stochastic systems: Part I, deterministic closures. *Comm. Math. Sci.*, 2:255–294, 2004.
- [9] M. A. Katsoulakis, A. J. Majda, and D. G. Vlachos. Coarse-grained stochastic processes and Monte Carlo simulations in lattice systems. *J. Comput. Phys.*, 186(1):250–278, 2003.
- [10] M. A. Katsoulakis, P. Plecháč, and A. Sopasakis. Error analysis of coarse-graining for stochastic lattice dynamics. *SIAM J. Num. Anal.*, 44(6), 2006.
- [11] S. Katz and J. Lebowitz and H. Spohn. Stationary nonequilibrium states for stochastic lattice gas models of ionic superconductors. *J. Statist. Phys.*, 34:497, 1984.
- [12] C. Kipnis and C. Landim. *Scaling Limits of Interacting Particle Systems*. Springer-Verlag, 1999.
- [13] J. Krug and H. Spohn. Universality classes for deterministic surface growth. *Phys. Rev. A*, 38:4271, 1988.
- [14] D. A. Kurtze and D. S. Hong. Traffic jams, granular flow, and soliton selection. *Phys. Rev. E*, 52:218–221, 1995.
- [15] T. M. Liggett. *Interacting Particle Systems*. Springer, 1985.
- [16] K. Nagel and M. Schreckenberg. A cellular automaton model for freeway traffic. *J. Phys. I France*, 2:2221, 1992.
- [17] I. Palasti. On some random space filling problems. *Publ. Math. Inst. Hungar. Acad. Sci.*, 5:353–360, 1960.
- [18] A. Renyi. On a one-dimensional problem concerning random space-filling. *Publ. Math. Inst. Hungar. Acad. Sci.*, 3:109–127, 1958.
- [19] M. Schreckenberg and D. E. Wolf. *Traffic and Granular Flow*. Springer Singapore, 1998.
- [20] T. P. Schulze. Efficient kinetic Monte Carlo simulation. *Journal of Computational Physics*, 227(4):2455–2462, February 2008.
- [21] A. Slepoy, A. P. Thompson, and S. J. Plimpton. A constant-time kinetic Monte Carlo algorithm for simulation of large biochemical reaction networks. *Journal of Chemical Physics*, 128(20):205101, 2008.
- [22] A. Sopasakis and M. A. Katsoulakis. Stochastic modeling and simulation of traffic flow: ASEP with Arrhenius look-ahead dynamics. *SIAM J. on Applied Mathematics*, 2005.

- [23] H. Spohn. Large scale dynamics of interacting particles. Springer-Verlag, 1991.
- [24] D. G. Vlachos and M. A. Katsoulakis. Derivation and validation of mesoscopic theories for diffusion of interacting molecules. *Phys. Rev. Let.*, 85(18):3898, 2000.
- [25] S. Wolfram, Cellular Automata as Simple Self-Organizing Systems, Caltech Preprint CALT-68-938 (submitted to Nature), 1982.
- [26] S. Wolfram, *A New Kind of Science*, Champaign, IL: Wolfram Media, Inc., 2002.
- [27] Z. Guo, C. Zheng, and B. Shi. Discrete lattice effects on the forcing term in the lattice Boltzmann method. *Phys. Rev. E*, 65(4):046308, 2002.